# Infrared Imaging of Nitric Oxide-Mediated Blood Flow in Human Sickle Cell Disease

**Alexander M. Gorbach**[a,1], **Hans C. Ackerman**[b,e,1,*], **Wei-Min Liu**[a], **Joseph M. Meyer**[a], **Patricia L. Littel**[c], **Catherine Seamon**[c], **Eleni Footman**[c], **Amy Chi**[c], **Suzana Zorca**[c], **Megan L. Krajewski**[c], **Michael J. Cuttica**[c,e], **Roberto F. Machado**[c,e], **Richard O. Cannon III**[d], and **Gregory J. Kato**[c,e]

[a]Infrared Imaging and Thermometry Unit, National Institute of Biomedical Imaging and Bioengineering [b]Laboratory of Malaria and Vector Research, National Institute of Allergy and Infectious Diseases [c]Sickle Cell Vascular Disease Section, both in the Cardiovascular and Pulmonary Branch, National Heart, Lung and Blood Institute [d]Clinical Cardiology Section, both in the Cardiovascular and Pulmonary Branch, National Heart, Lung and Blood Institute [e]Critical Care Medicine Department, Clinical Center—all at the National Institutes of Health in Maryland

## Abstract

Vascular dysfunction is an important pathophysiologic manifestation of sickle cell disease (SCD), a condition that increases risk of pulmonary hypertension and stroke. We hypothesized that infrared (IR) imaging would detect changes in cutaneous blood flow reflective of vascular function. We performed IR imaging and conventional strain gauge plethysmography in twenty-five adults with SCD at baseline and during intra-arterial infusions of an endothelium-dependent vasodilator acetylcholine (ACh), an endothelium-independent vasodilator sodium nitroprusside (SNP), and a NOS inhibitor L-NMMA. Skin temperature measured by IR imaging increased in a dose-dependent manner to graded infusions of ACh ($+1.1°$ C, $p < 0.0001$) and SNP ($+0.9°$ C, $p < 0.0001$), and correlated with dose-dependent increases in forearm blood flow (ACh: $+19.9$ mL/min/100mL, $p < 0.0001$; $r_s = 0.57$, $p = 0.003$; SNP: $+8.6$ mL/min/100mL, $p < 0.0001$; $r = 0.70$, $p = 0.0002$). Although IR measurement of skin temperature accurately reflected agonist-induced increases in blood flow, it was less sensitive to decreases in blood flow caused by NOS inhibition. Baseline forearm skin temperature measured by IR imaging correlated significantly with baseline forearm blood flow ($31.8\pm0.2°$ C, $6.0\pm0.4$ mL/min/100mL; $r = 0.58$, $p = 0.003$), and appeared to represent a novel biomarker of vascular function. It predicted a blunted blood flow response to SNP ($r = -0.61$, $p = 0.002$), and was independently associated with a marker of pulmonary artery pressure, as well as hemoglobin level, diastolic blood pressure, homocysteine, and cholesterol ($R^2 = 0.84$, $p < 0.0001$ for the model). IR imaging of agonist-stimulated cutaneous blood flow represents a less cumbersome alternative to plethysmography methodology. Measurement of

*Corresponding author: Hans Ackerman, M.D., D.Phil., Laboratory of Malaria and Vector Research, 12735 Twinbrook Parkway, Rockville, Maryland 20852, Tel: (301) 728-9148, Fax: (301) 480-0930, hans.ackerman@nih.gov.
[1]Equal contributors.

*Present affiliations.* PLL: Laboratory of Host Defenses, National Institute of Allergy and Infectious Diseases, Bethesda, Maryland; MLK: Departement of Anesthesiology, Perioperative and Pain Medicine, Brigham and Women's Hospital 75 Francis Street, Boston, Massachusetts; MJC: Division of Pulmonary and Critical Care Medicine, Feinberg School of Medicine, Northwestern University, Chicago, Illinois; RFM: Section of Pulmonary, Critical Care Medicine, Sleep and Allergy, University of Illinois, Chicago, Illinois.

baseline skin temperature by IR imaging may be a useful new marker of vascular risk in adults with SCD.

**Keywords**

Plethysmography; Sickle cell; Temperature; Endothelium; Smooth muscle; Skin; Hemoglobin; Acetylcholine; Nitroprusside; L-NMMA

## 1. Introduction

Sickle cell disease is a chronic hemolytic anemia caused by a homozygous amino acid substitution in the beta chain of hemoglobin (Ingram, 1957). Polymerization of deoxygenated hemoglobin S inside red blood cells impairs their deformability and triggers vaso-occlusive events (Pauling et al., 1949; Chien et al., 1982; Embury, 1986). Individuals with sickle cell disease are at increased risk for stroke (Ohene-Frempong et al., 1998), pulmonary hypertension (Collins and Orringer, 1982; Castro et al., 2003; Anthi et al., 2007; Parent et al., 2011), and renal dysfunction (Powars et al., 1991)—possibly due to organ-specific manifestations of systemic vascular disease (Morris, 2011).

Vascular dysfunction is common among patients with sickle cell disease and has been documented using several different modalities for assessing vascular physiology. Vasodilation triggered by shear stress, an endothelium-dependent response, is diminished in patients with sickle cell disease as measured by brachial artery ultrasonography or by digital plethysmography (de Montalembert et al., 2007; Belhassen et al., 2001; Sivamurthy et al., 2009). Diminished NO synthesis from depletion of arginine or competitive inhibition by methylated arginine may contribute to endothelial dysfunction (Morris et al., 2005; Kato et al., 2009; Landburg et al., 2010). In addition to endothelial dysfunction, sickle cell patients also demonstrate diminished vasodilatory responses to nitric oxide donors such as sodium nitroprusside or nitroglycerin (Reiter et al., 2002; Eberhardt et al., 2003), agents that directly stimulate vascular smooth muscle relaxation via soluble guanylate cyclase. This has been attributed to vascular smooth muscle dysfunction or to functional nitric oxide resistance whereby a fraction of exogenous nitric oxide is scavenged by reactive oxygen species or extracellular heme before it can stimulate vascular smooth muscle (Huie and Padmaja, 1993; Aslan et al., 2001). More informative techniques are needed to elucidate the pathophysiologic mechanisms of vascular dysfunction in sickle cell disease.

The skin provides an accessible vascular bed for the study of blood flow and vascular function. Disturbances in cutaneous blood flow may reflect pathophysiological changes in other important organ systems (Holowatz et al., 2008). Whereas many studies have used skin heating and cooling to stimulate vasodilation and vasoconstriction, we take the converse approach of administering intra-arterial vasodilators and vasoconstrictors and measuring the skin temperature response. In a typical indoor environment, blood is warmer than surrounding skin tissue, creating a temperature gradient amenable to accurate and quantitative detection by infrared imaging. We hypothesized that forearm skin temperature would correlate with forearm blood flow. We determined the relationship between forearm skin temperature and total cross-sectional forearm blood flow by acquiring infrared images of the forearm while simultaneously performing conventional strain gauge venous occlusion plethysmography. We further characterized the regulation of skin temperature and blood flow by sequentially infusing endothelium-dependent and endothelium-independent vasodilators and a nitric oxide synthase inhibitor into the brachial artery of each subject. We find that skin temperature is correlated with blood flow in response to vasodilators, but not

vasoconstrictors. We also present preliminary data that warmer basal skin temperature is associated with impaired nitric oxide-mediated smooth muscle relaxation.

## 2. Materials and Methods

### 2.1. Subjects

Adult subjects with sickle cell anemia provided written informed consent in accordance with the Declaration of Helsinki and were enrolled at the NIH Clinical Center on clinical protocol NIH 07-H-0196 specifically approved for this study by the Institutional Review Board of the National Heart, Lung and Blood Institute. Subjects were included if they were between 18 and 65 years of age, diagnosed with sickle cell disease by hemoglobin electrophoresis or HPLC, and had a total hemoglobin concentration greater than 5.5 g/dL. Additional inclusion criteria were apolipoprotein A-I less than 99 mg/dL or high density lipoprotein cholesterol less than 39 mg/dL, factors that may increase the risk of endothelial dysfunction in sickle cell patients (Yuditskaya et al., 2009). Subjects with pain crisis, pregnancy or hemoglobin SC disease were excluded from this study. Subjects were excluded if they had other conditions (diabetes, hypertension, renal insu ciency, hyperuricemia, coronary artery disease, peripheral arterial disease or smoking) or took medications (aspirin, NSAIDs, PDE-5 inhibitors, arginine, fibrates, statins, prostaglandins) that affect endothelial function.

Each subject's temperature was measured by trained research nurses using a tympanic membrane thermometer (Model AccuSystem Genius 2, Tyco Healthcare Group LP, USA) that was calibrated against a Genius 2 blackbody certified and traceable to the National Institute of Standards and Technology (NIST). Venous blood samples were drawn for clinical laboratory tests (Table 1).

### 2.2. Administration of Vasoactive Infusions

Figure 1 illustrates the study procedures. During a 20-minute period of equilibration in a temperature controlled room (22-24°C), each subject had room temperature 0.9% sodium chloride infused through a brachial artery catheter at 1 mL/min. This was followed by 6-minute infusions of escalating doses of acetylcholine at 7.5, 15, and 30 $\mu$g/min to assess endothelium-dependent forearm blood flow. After ACh infusions, each subject underwent a 40-minute re-equilibration period during which 0.9% sodium chloride was infused again at 1 mL/min. This was followed by a dose escalation of sodium nitroprusside (SNP) at 0.8, 1.6, and 3.2 $\mu$g/min to assess endothelium-independent forearm blood flow, a 30-minute 0.9% sodium chloride infusion at 1 mL/min, and finally an infusion of L-$N^G$-monomethyl Arginine (L-NMMA) at 4 $\mu$mol/min to assess the role of nitric oxide synthase in regulating forearm blood flow.

### 2.3. Infrared Image Analysis

The cooled infrared camera (Santa Barbara FocalPlane Array, Lockheed Martin, USA) was positioned at a distance 90 cm above the subject's arm which was placed in a cradle to minimize involuntary movements. Infrared images with 320×256 pixels per frame were acquired in the 3.0-5.0 $\mu$m wavelength specturm at 2 Hz using WinIR software (Lockheed Martin, USA). An emissivity of 0.958 was used as recommended for 3.0-5.0 $\mu$m wavelengths (Hassan et al., 2007). The infrared camera was calibrated once every three months (11-point calibration with 0.5°C steps within 28 - 33°C temperature range) against a blackbody calibration unit (model SR80 Extended Area Infrared Radiation Source, CI Systems, Israel) with 0.01°C temperature resolution and 0.001°C readout resolution at near-ambient temperature. Estimated accuracy of the infrared camera was within ±0.1°C. The stability of temperature measurements was better than ±0.04°C over one hour. This camera can resolve two adjacent pixels that di er by 0.015°C.

A rigid-body image alignment algorithm was applied to the infrared images to minimize motion artifact. For each subject, the medial aspect of the forearm between the wrist cuff and the upper arm cuff was circumscribed to define the region of interest. Forearm temperature was averaged over the region of interest and plotted with respect to time (see example in Figure 2). During infusion of the vasodilators ACh and SNP, forearm skin temperature rose, and the maximum temperature achieved during each drug dose was analyzed. During infusion of the vasoconstrictor L-NMMA, forearm skin temperature fell, and the minimum temperature achieved during the L-NMMA infusion was analyzed.

### 2.4. Forearm Blood Flow Analysis

Forearm blood flow was measured using the AI6 Arterial Inflow system (Hokanson, Bellevue, Washington) that uses a strain gauge plethysmograph to measure forearm distension after occlusion of venous return. Venous occlusion was achieved with automated upper arm cuff inflation to 40 mm Hg, and the effects of shunting in the hand were eliminated by automated inflation of an occlusive wrist cuff.

Seven replicate plethysmographic measurements of forearm distension during venous occlusion were taken before each dose escalation at time points 0.5, 8.5, 16.5, and 24.5 minutes. Each plot of forearm circumference versus time was manually inspected by a single investigator and a line was fitted to represent blood flow. Blood flow was normalized to forearm volume and presented as mL / minute / 100 mL of forearm tissue. The mean of seven replicates was used in subsequent analyses.

### 2.5. Echocardiography

Transthoracic echocardiography was performed in all patients using the Acuson Sequoia (Siemens-Acuson, Mountain View, CA) and the Sonos 5500 (Philips, Andover, MA). Tricuspid regurgitation velocity was assessed in the parasternal right ventricular inflow, parasternal short axis, and apical four-chamber views, and a minimum of five sequential complexes were recorded using continuous wave Doppler sampling. This measurement has been shown to correlate with pulmonary artery systolic pressure in the absence of right ventricular outflow obstruction and pulmonic stenosis (Berger et al., 1985). This technique has been compared with pulmonary artery catheterization in patients with SCD (Gladwin et al., 2004).

### 2.6. Statistical Analysis

Forearm blood flow, forearm skin temperature, and tympanic membrane temperature are presented as mean ± standard error. Forearm blood flow and forearm skin temperature were plotted as the mean and standard error with respect to drug dose. Changes in skin temperature or blood flow were analyzed with the paired $t$-test, Mann-Whitney U test or analysis of variance with repeated measures. Correlations were analyzed by Spearman's or Pearson's correlation test. Area under the curve (AUC) was calculated using the trapezoidal rule with subtraction of the area below the baseline blood flow or temperature. When temperature or blood flow decreased, the AUC was negative. The AUC units are the product of the $x$ and $y$ axes in Figure 3: °C-$\mu$g/min and mL/min/100ml tissue-$\mu$g/min. AUC was calculated for each dose interval (7.5 $\mu$g/min of ACh, or 0.8 $\mu$g/min of SNP) and the sum of all three doses was calculated. For this reason, the units are °C-7.5$\mu$g/min and mL/min/100ml tissue-7.5$\mu$g/min for ACh, °C-0.8$\mu$g/min and mL/min/100ml tissue-0.8$\mu$g/min for SNP, and °C-4$\mu$mol/min and mL/min/100ml tissue-4$\mu$mol/min for L-NMMA. In the article text, this is abbreviated as °C-$\mu$g/min and mL/min/100ml tissue-$\mu$g/min, and in the figures it is abbreviated as AUC. The correlation between blood flow AUC and temperature AUC was calculated using Spearman's method.

Multivariable linear regression was used to identify patient characteristics that were associated with baseline forearm skin temperature. The model was built by first including any variable that was correlated with baseline forearm skin temperature with a $p$-value less than 0.15. Variables were removed from the model if they did not contribute significantly to the multivariable model (individual $p$-values greater than 0.05). The final minimum model is presented in Table 2 which lists the standardized estimate and the p-value for each variable as well as $R^2$, $F$, and the $p$-value for the final model.

## 3. Results

### 3.1. Baseline Characteristics of the Research Subjects

Twenty-five subjects underwent both infrared imaging and conventional forearm blood flow measurements by venous occlusion strain gauge plethysmography (see Figure 1 for an illustration of the study design). The mean age of the subjects was 28 years, and there were 10 females (40 %). The characteristics of the study population are provided in Table 1.

Core temperature measured at the tympanic membrane was 36.9±0.1°C. Baseline forearm skin temperature measured by infrared imaging was 31.8±0.2°C and was correlated with the baseline forearm blood flow (6.0 ± 1.8 mL/min/100 mL tissue) measured by conventional strain gauge venous occlusion plethysmography ($r = 0.58$, $p = 0.003$; Figure 3).

### 3.2. Temperature and Blood Flow Responses to the Endothelium-Dependent Vasodilator Acetylcholine

Forearm skin temperature measured by infrared imaging was 31.8±0.2°C at baseline and rose in a dose-dependent manner during three escalating doses of intra-arterial acetylcholine (ACh) (32.4±0.2, 32.6±0.2, 32.9±0.2°C, $p < 0.001$ for each interval; Figure 4A)). During the highest infusion rate of ACh, 30 $\mu$g/min, forearm skin temperature increased by 1.1 ± 0.2°C over baseline ($p < 0.0001$). Changes in the forearm skin temperature were visually apparent in the infrared images recorded during ACh infusion compared to saline control infusion (Figure 2).

Plethysmographic measurements of forearm blood flow were recorded for each dose of ACh. Forearm blood flow at baseline was 6.0±0.4 mL/min/100 mL tissue and increased with each escalating dose of ACh (16.4 ± 1.3, 20.4 ± 1.8, 25.9 ± 2.3 mL/min/100 mL tissue; $p < 0.001$ for each interval; Figure 4B). At maximal dose ACh, forearm blood flow increased by 19.9 ± 2.3 mL/min/100 mL tissue over baseline ($p < 0.0001$).

The area under the dose-response curve was 2.9 ± 0.5°C-$\mu$g/min and 52.0 ± 5.8 mL/min/100ml tissue-$\mu$g/min for temperature and blood flow responses to ACh, respectively, and the two measurements were correlated ($r_s = 0.57$, $p = 0.003$; Figure 4C).

### 3.3. Temperature and Blood Flow Responses to the Endothelium-Independent Vasodilator Sodium Nitroprusside

After a subsequent 40-minute infusion of room-temperature saline at 1 mL/min, baseline forearm skin temperature was 32.2 ± 0.2°C. Escalating doses of SNP at 0.8, 1.6, and 3.2 $\mu$g/min caused a dose-dependent increase in skin temperature (32.4 ± 0.2, 32.6 ± 0.2, 33.0 ± 0.1°C; $p < 0.0001$ for each interval). At maximal dose SNP, skin temperature increased by 0.9 ± 0.1°C over baseline ($p < 0.0001$; Figure 4D).

Forearm blood flow at baseline was 6.5 ± 0.3 mL/min/100 mL tissue and increased with each dose escalation of SNP (9.3 ± .3, 11.6 ± 0.6, 15.1 ± 0.9 mL/min/100 mL; $p < 0.0001$

for each interval) achieving a maximum increase of $8.6 \pm 1.0$ mL/min/100 mL tissue over baseline ($p < 0.0001$; Figure 4E).

The area under the dose-response curve was $1.9 \pm 0.3°C$-$\mu$g/min and $19.0 \pm 2.5$ mL/min/ 100ml tissue-$\mu$g/min for temperature and blood flow responses to SNP, respectively, and the two measurements were correlated ($r = 0.70$, $p = 0.0002$; Figure 4F).

At maximum dose SNP, the increase in skin temperature ($+0.9 \pm 0.1°C$) was similar to the increase seen with maximum dose ACh ($+1.1 \pm 0.2°C$) despite a lower blood flow response to SNP compared to ACh ($8.6 \pm 1.0$ versus $19.9 \pm 2.3$). The increase of skin temperature relative to the increase of blood flow was significantly greater for SNP than for ACh ($p = 0.02$ by two-way ANOVA; Figure 6)

### 3.4. Temperature and Blood Flow Responses to Nitric Oxide Synthase Inhibition by L-N$^G$-Monomethyl Arginine

Following a 30-minute infusion of room-temperature saline at 1 mL/min, baseline forearm skin temperature was $32.2 \pm 0.2°C$. After five minutes of infusion of 4 $\mu$mol/min intra-arterial L-$N^G$-monomethyl arginine (L-NMMA), a nitric oxide synthase (NOS) inhibitor, forearm skin temperature fell to $31.8 \pm 0.2°C$ ($p < 0.0001$; Figure 4G). This decrease of $0.3°C$ below baseline indicates a role for NOS activity in regulating basal skin temperature.

Mean forearm blood flow at baseline was $6.9 \pm 0.4$ mL/min/100 mL tissue and decreased to $5.4 \pm 0.4$ mL/min/100 mL tissue after five minutes of infusion of 4 $\mu$mol/min L-NMMA ($p < 0.0001$; Figure 4H). This indicates that $22 \pm 3.5\%$ or more of baseline blood flow was NOS-dependent.

The area under the dose-response curves was $-0.16 \pm 0.02°C$-$\mu$g/min and $-0.76 \pm 0.12$ mL/ min/100ml tissue-$\mu$g/min for temperature and blood flow responses to the vasoconstrictor L-NMMA, respectively, but the two measurements were not correlated ($r = 0.06$, $p = 0.80$; Figure 4I).

### 3.5. Baseline Forearm Skin Temperature and the Response to Vasodilator Infusions

Baseline forearm skin temperature, measured before administration of each vasoactive drug, provided several significant inverse correlations with the response to vasodilator drug infusions, especially in response to SNP (Figure 5). The forearm skin temperature response to SNP inversely correlated with the baseline forearm skin temperature ($r = -0.70$, $p = 0.0001$, Figure 5D); furthermore, the forearm blood flow response to SNP was inversely correlated with the baseline forearm blood flow ($r = -0.605$, $p = 0.0017$, Figure 5E). In a comparison across modalities, baseline forearm skin temperature, measured by infrared imaging before the administration of SNP, was predictive of the blood flow response to SNP measured by strain gauge plethysmography ($r = -0.611$, $p = 0.0015$, Figure 5F). Subjects with warmer skin at baseline tended to have diminished augmentation of forearm blood flow in response to the intra-arterial infusion of sodium nitroprusside.

We observed less significant associations of baseline skin temperature with ACh responses. The forearm skin temperature response to ACh was inversely correlated with the baseline forearm skin temperature ($r = -0.42$, $p = 0.039$, Figure 5A); however, there was no correlation between the forearm blood flow response to ACh and the baseline forearm blood flow ($p = 0.79$, Figure 5B). In the comparison across modalities, the blood flow response to ACh was not correlated with the baseline forearm skin temperature ($p = 0.45$, Figure 5C).

### 3.6. Patient Characteristics Associated with Baseline Forearm Skin Temperature

To better understand the inverse correlation between baseline forearm skin temperature and the blood flow response to sodium nitroprusside, we used multivariable linear regression to identify patient characteristics that were independently associated with the baseline forearm skin temperature measured before any vasoactive infusions were administered. Anemia is known to increase the tricuspid valve regurgitant velocity (TRV) (Dham et al., 2009) and so a term for this significant interaction was included in the model. Diastolic blood pressure and TRV were positively associated with baseline skin temperature, while hemoglobin concentration, serum homocysteine concentration and serum total cholesterol were negatively associated with baseline forearm skin temperature (Table 2, $R^2 = 0.84$, $F = 12.6$, $p < 0.0001$ for the model).

## 4. Discussion

Patients with sickle cell disease are at increased risk for vascular diseases such as stroke, pulmonary hypertension, and renal dysfunction. In an effort to develop new technologies to assess vascular dysfunction in patients with sickle cell disease, we compared forearm skin temperature measured by infrared imaging against forearm blood flow measured by conventional strain gauge plethysmography. We found that forearm skin temperature was strongly correlated with forearm blood flow not only at baseline, but also in response to the endothelium-dependent and endothelium-independent vasodilators ACh and SNP. Unexpectedly, we found that warm baseline skin temperature was associated with diminished responsiveness to these vasodilators.

The most striking relationship was observed in response to the infusion of an NO donor, SNP, where warm baseline forearm skin temperature (measured by infrared imaging) and high baseline forearm blood flow (measured by strain gauge plethysmography) were both associated with a diminished vasodilatory response. Resistance to NO-mediated vasodilation has been previously observed in both animal models and humans with sickle cell disease (Kaul et al., 2000, 2004; Eberhardt et al., 2003; Nath et al., 2000), but never before has it been related to basal skin temperature. Some of the proposed mechanisms of resistance to NO-mediated vasodilation include increased consumption of NO or decreased activity of soluble guanylate cyclase and other downstream messengers in vascular smooth muscle (Gladwin and Kato, 2005). In this study, we have identified baseline skin temperature as a new preliminary predictor of NO responsiveness.

Interestingly, the endothelium-independent and endothelium-dependent vasodilators (SNP and ACh) both elicited a similar increase in skin temperature ($0.9 \pm 0.1°$ and $1.1 \pm 0.2°$, respectively) despite SNP stimulating a much smaller cross-sectional forearm blood flow response ($8.6 \pm 1.0$ vs $19.9 \pm 2.3$ mL/min/100mL). Since infrared imaging is most sensitive to surface blood flow, and strain gauge plethysmography measures total blood flow (surface plus conduit vessels), we can speculate that SNP stimulated skin blood flow to a greater extent than conduit blood flow, relative to ACh. This observation would be consistent with a model of microvascular endothelial dysfunction, where small vessels of the skin respond appropriately to the smooth muscle relaxant SNP, but have impaired responses to the endothelium-dependent vasodilator ACh. An alternative interpretation of these data is that the thermal response to both vasodilators was constrained by a skin temperature ceiling of approximately 33°C, and the additional blood flow elicited by ACh was carried by conduit vessels. Evidence for a skin temperature ceiling (or minimum difference between core and surface temperatures) was recently provided by a study involving strenuous exercise in a warm, humid environment. Skin temperature remained more than 4°C cooler than core body temperature, despite significant elevations of core body temperatures induced by exercise. Skin temperature only exceeded 33°C when core body temperature rose above 37°

(Maughan et al., 2011). However, in our study, there was no direct evidence for a skin thermal response ceiling; we observed significant increases in skin temperature after each increase in vasodilator dose over a four-fold range.

We considered whether high baseline forearm skin temperature was associated with any existing risk factors for vascular complications of sickle cell disease. Baseline skin temperature was positively associated with the tricuspid valve regurgitant velocity (TRV). Elevated TRV is a marker of pulmonary vasculopathy and is associated with increased early mortality in adults with sickle cell disease (Gladwin et al., 2004; Anthi et al., 2007; Parent et al., 2011; Fonseca et al., 2012). We also found warm baseline skin temperature to be associated with the degree of anemia, another established marker of disease severity in sickle cell patients. One interpretation of these findings is that anemia leads to a compensatory increase in cardiac output, which contributes to both higher TRV(Dham et al., 2009) and greater perfusion of the skin at baseline.

Increased blood flow in vascular beds other than skin has previously been associated with vascular complications of sickle cell disease. For example, increased blood flow in the large intracranial arteries is predictive of stroke among children with sickle cell disease even in the absence of cerebrovascular stenosis (Adams et al., 1997). This observation has led to the current standard of care clinical practice of measuring blood flow velocity in the intracranial arteries by transcranial Doppler ultrasonography to identify children at high risk for stroke, and to guide e ective prophylactic therapy (Adams et al., 1998). Increased renal blood flow has been associated with glomerulomegaly and development of renal insu ciency in patients with sickle cell disease (Etteldorf et al., 1952; Bernstein and Whitten, 1960; Hatch et al., 1970). Outside of sickle cell disease, in patients with congenital heart disease, excessive pulmonary blood flow contributes to the development of pulmonary hypertension (Beghetti and Tissot, 2009). Our results suggest that the skin may be another vascular bed where pathophysiological increases in baseline blood flow can be observed. This preliminary observation might encourage further investigation into the potential of baseline forearm skin temperature to serve as a simple physiological biomarker of vascular risk in sickle cell patients.

Our study has several limitations. We performed these studies exclusively in subjects with sickle cell disease, in an effort to identify individuals with sickle cell disease who have impaired vascular function and may be at risk for adverse events. We used appropriate within-group analyses such as correlation analysis, analysis of variance, and linear regression that do not require comparison with a control group; however, our observations cannot be extrapolated to healthy individuals. In order to carry out a complicated study procedure accurately and reproducibly, we did not randomize the order of the vasoactive infusions. This could induce bias if one drug had an effect on the next; however these drugs have short half-lives, there was a wash-out period between infusions, and the skin temperatures before the start of each infusion did not differ significantly. Finally, we observed blood flow in the forearm and temperature of the skin, but how this relates to blood flow in other organs such as the brain or kidney was not assessed. With twenty-five subjects, we had a statistical power of 80% to detect a correlation of $r = 0.5$ or greater at the $p < 0.05$ threshold. Correlations less than $r = 0.50$ may not have been detected.

We observed significant correlations between forearm blood flow and skin temperature while vasodilators were administered, but not while the vasoconstrictor L-NMMA was administered. This could be explained by different mechanisms of skin warming and skin cooling. Skin temperature can be changed by increasing or decreasing the inflow of warmer blood: when the inflow of warmer blood is increased, temperature rises immediately; however, when the inflow of warmer blood is decreased, temperature only begins to fall

once passive mechanisms such as radiation, evaporation, conduction and air convection remove heat from the skin surface. An extreme example of this is the thermal response to brachial artery occlusion and release; the cooling phase that occurs after brachial artery occlusion is gradual even though arterial blood flow has ceased (McQuilkin et al., 2009). During the re-warming phase after release of the occlusion, both skin temperature and arterial blood flow increase rapidly. This illustrates the discordance between blood flow and skin temperature after a vasoconstrictor is administered and exposes a limitation of infrared imaging to detect sudden decreases in blood flow.

Despite this limitation, infrared imaging does offer several technical advantages for the assessment of blood flow in clinical studies. It is non-invasive and relies on passive radiation of infrared energy; there is no transmission of energy or radiation to the subject. Standard venous-occlusion plethysmography perturbs the vascular bed under observation by indentation of the skin with a silastic strain gauge and intermittent occlusion of venous blood flow return from the upper limb and arterial blood flow to the hand by pneumatic cuff inflations. In contrast, infrared imaging requires no contact of the detector with the skin, minimizing potential disturbances to the microcirculation under observation. Infrared imaging allows for nearly continuous image acquisition over time, a feature that would support the quantitative analysis of responses to a vasoactive drugs, reactive hyperemia, or cutaneous blood vessel recruitment.

In summary, infrared imaging technology provides a useful, non-invasive alternative to conventional gold-standard methodology of strain gauge venous occlusion plethysmography, as seen in this clinical investigation of blood flow in human sickle cell disease. This methodology has provided preliminary evidence that basal skin temperature might predict vasodilatory response to an NO donor in adults with sickle cell disease. These findings illustrate the potential of infrared imaging to advance our understanding of vascular dysfunction in sickle cell disease.

## Acknowledgments

## References

Adams R, McKie V, Hsu L, Files B, Vichinsky E, Pegelow C, Abboud M, Gallagher D, Kutlar A, Nichols F, Bonds D, Brambilla D. Prevention of a first stroke by transfusions in children with sickle cell anemia and abnormal results on transcranial doppler ultrasonography. N Engl J Med. 1998; 339:5–11. [PubMed: 9647873]

Adams RJ, McKie VC, Carl EM, Nichols FT, Perry R, Brock K, McKie K, Figueroa R, Litaker M, Weiner S, Brambilla D. Long-term stroke risk in children with sickle cell disease screened with transcranial doppler. Ann Neurol. 1997; 42:699–704. [PubMed: 9392568]

Anthi A, Machado R, Jison M, Taveira-Dasilva A, Rubin L, Hunter L, Hunter C, Coles W, Nichols J, Avila N, Sachdev V, Chen C, Gladwin M. Hemodynamic and functional assessment of patients with sickle cell disease and pulmonary hypertension. Am J Respir Crit Care Med. 2007; 175:1272–9. [PubMed: 17379852]

Aslan M, Ryan T, Adler B, Townes T, Parks D, Thompson J, Tousson A, Gladwin M, Patel R, Tarpey M, Batinic-Haberle I, White C, Freeman B. Oxygen radical inhibition of nitric oxide-dependent vascular function in sickle cell disease. Proc Natl Acad Sci U S A. 2001; 98:15215–20. [PubMed: 11752464]

Beghetti M, Tissot C. Pulmonary arterial hypertension in congenital heart diseases. Semin Respir Crit Care Med. 2009; 30:421–8. [PubMed: 19634081]

Belhassen L, Pelle G, Sediame S, Bachir D, Carville C, Bucherer C, Lacombe C, Galacteros F, Adnot S. Endothelial dysfunction in patients with sickle cell disease is related to selective impairment of shear stress-mediated vasodilation. Blood. 2001; 97:1584–9. [PubMed: 11238095]

Berger M, Haimowitz A, Tosh AV, Berdo RL, Goldberg E. Quantitative assessment of pulmonary hypertension in patients with tricuspid regurgitation using continuous wave doppler ultrasound. J Am Coll Cardiol. 1985; 6:359–65. [PubMed: 4019921]

Bernstein J, Whitten C. A histologic appraisal of the kidney in sickle cell anemia. Arch Pathol. 1960; 70:407–18. [PubMed: 13868273]

Castro O, Hoque M, Brown B. Pulmonary hypertension in sickle cell disease: cardiac catheterization results and survival. Blood. 2003; 101:1257–61. [PubMed: 12393669]

Chien S, King RG, Kaperonis AA, Usami S. Viscoelastic properties of sickle cells and hemoglobin. Blood Cells. 1982; 8:53–64. [PubMed: 7115978]

Collins F, Orringer E. Pulmonary hypertension and cor pulmonale in the sickle hemoglobinopathies. Am J Med. 1982; 73:814–21. [PubMed: 7148875]

Dham N, Ensing G, Minniti C, Campbell A, Arteta M, Rana S, Darbari D, Nouraie M, Onyekwere O, Lasota M, Kato GJ, Gladwin MT, Castro O, Gordeuk V, Sable C. Prospective echocardiography assessment of pulmonary hypertension and its potential etiologies in children with sickle cell disease. Am J Cardiol. 2009; 104:713–20. [PubMed: 19699350]

Eberhardt R, McMahon L, Du y S, Steinberg M, Perrine S, Loscalzo J, Co man J, Vita J. Sickle cell anemia is associated with reduced nitric oxide bioactivity in peripheral conduit and resistance vessels. Am J Hematol. 2003; 74:104–11. [PubMed: 14508796]

Embury SH. The clinical pathophysiology of sickle cell disease. Annu Rev Med. 1986; 37:361–76. [PubMed: 2423018]

Etteldorf JN, Tuttle AW, Clayton GW. Renal function studies in pediatrics. 1. renal hemodynamics in children with sickle cell anemia. AMA Am J Dis Child. 1952; 83:185–91. [PubMed: 14884754]

Fonseca GHH, Souza R, Salemi VMC, Jardim CVP, Gualandro SFM. Pulmonary hypertension diagnosed by right heart catheterisation in sickle cell disease. Eur Respir J. 2012; 39:112–8. [PubMed: 21778170]

Gladwin M, Kato G. Cardiopulmonary complications of sickle cell disease: role of nitric oxide and hemolytic anemia. Hematology. 2005:51–7. [PubMed: 16304359]

Gladwin M, Sachdev V, Jison M, Shizukuda Y, Plehn J, Minter K, Brown B, Coles W, Nichols J, Ernst I, Hunter L, Blackwelder W, Schechter A, Rodgers G, Castro O, Ognibene F. Pulmonary hypertension as a risk factor for death in patients with sickle cell disease. N Engl J Med. 2004; 350:886–95. [PubMed: 14985486]

Hassan, M.; Chernomordik, V.; Vogel, A.; Hattery, D.; Gannot, I.; Little, R.; Yarchoan, R.; Gandjbakhche, A. Infrared imaging for functional monitoring of disease processes. In: Diakides, N.; Bronzino, J., editors. Medical Infrared Imaging. CRC Press; USA: 2007. p. 14-17.chapter 14

Hatch FE, Azar SH, Ainsworth TE, Nardo JM, Culbertson JW. Renal circulatory studies in young adults with sickle cell anemia. J Lab Clin Med. 1970; 76:632–40. [PubMed: 5458026]

Holowatz LA, Thompson-Torgerson CS, Kenney WL. The human cutaneous circulation as a model of generalized microvascular function. J Appl Physiol. 2008; 105:370–2. [PubMed: 17932300]

Huie RE, Padmaja S. The reaction of no with superoxide. Free Radic Res Commun. 1993; 18:195–9. [PubMed: 8396550]

Ingram VM. Gene mutations in human haemoglobin: the chemical di erence between normal and sickle cell haemoglobin. Nature. 1957; 180:326–8. [PubMed: 13464827]

Kato GJ, Wang Z, Machado RF, Blackwelder WC, Taylor JG, Hazen SL. Endogenous nitric oxide synthase inhibitors in sickle cell disease: abnormal levels and correlations with pulmonary hypertension, desaturation, haemolysis, organ dysfunction and death. Br J Haematol. 2009; 145:506–13. [PubMed: 19344390]

Kaul D, Liu X, Chang H, Nagel R, Fabry M. E ect of fetal hemoglobin on microvascular regulation in sickle transgenic-knockout mice. J Clin Invest. 2004; 114:1136–45. [PubMed: 15489961]

Kaul D, Liu X, Fabry M, Nagel R. Impaired nitric oxide-mediated vasodilation in transgenic sickle mouse. Am J Physiol Heart Circ Physiol. 2000; 278:H1799–806. [PubMed: 10843875]

Landburg PP, Teerlink T, Biemond BJ, Brandjes DPM, Muskiet FAJ, Duits AJ, Schnog JB, study group, C. Plasma asymmetric dimethylarginine concentrations in sickle cell disease are related to the hemolytic phenotype. Blood Cells Mol Dis. 2010; 44:229–32. [PubMed: 20185345]

Maughan RJ, Otani H, Watson P. Influence of relative humidity on prolonged exercise capacity in a warm environment. Eur J Appl Physiol. 2011:1–9.

McQuilkin, GL.; Panthagani, D.; Metcalfe, RW.; Hassan, H.; Yen, AA.; Naghavi, M.; Hartley, CJ. Digital thermal monitoring (dtm) of vascular reactivity closely correlates with doppler flow velocity; Conference proceedings: Annual International Conference of the IEEE Engineering in Medicine and Biology Society IEEE Engineering in Medicine and Biology Society Conference; 2009; 2009. p. 1100-3.

de Montalembert M, Aggoun Y, Niakate A, Szezepanski I, Bonnet D. Endothelial-dependent vasodilation is impaired in children with sickle cell disease. Haematologica. 2007; 92:1709–10. [PubMed: 18055999]

Morris C, Kato G, Poljakovic M, Wang X, Blackwelder W, Sachdev V, Hazen S, Vichinsky E, Morris S, Gladwin M. Dysregulated arginine metabolism, hemolysis-associated pulmonary hypertension, and mortality in sickle cell disease. JAMA. 2005; 294:81–90. 1538-3598 Journal Article. [PubMed: 15998894]

Morris CR. Vascular risk assessment in patients with sickle cell disease. Haematologica. 2011; 96:1–5. [PubMed: 21193426]

Nath K, Shah V, Haggard J, Croatt A, Smith L, Hebbel R, Katusic Z. Mechanisms of vascular instability in a transgenic mouse model of sickle cell disease. Am J Physiol Regul Integr Comp Physiol. 2000; 279:R1949–55. [PubMed: 11080057]

Ohene-Frempong K, Weiner S, Sleeper L, Miller S, Embury S, Moohr J, Wethers D, Pegelow C, Gill F. Cerebrovascular accidents in sickle cell disease: rates and risk factors. Blood. 1998; 91:288–94. [PubMed: 9414296]

Parent F, Bachir D, Inamo J, Lionnet F, Driss F, Loko G, Habibi A, Bennani S, Savale L, Adnot S, Maitre B, Yäici A, Hajji L, O'Callaghan DS, Clerson P, Girot R, Galacteros F, Simonneau G. A hemodynamic study of pulmonary hypertension in sickle cell disease. N Engl J Med. 2011; 365:44–53. [PubMed: 21732836]

Pauling L, Itano HA, Singer S, Wells I. Sickle cell anemia a molecular disease. Science. 1949; 110:543–8. [PubMed: 15395398]

Powars DR, Elliott-Mills DD, Chan L, Niland J, Hiti AL, Opas LM, Johnson C. Chronic renal failure in sickle cell disease: risk factors, clinical course, and mortality. Ann Intern Med. 1991; 115:614–20. [PubMed: 1892333]

Reiter CD, Wang X, Tanus-Santos JE, Hogg N, Cannon RO, Schechter AN, Gladwin MT. Cell-free hemoglobin limits nitric oxide bioavailability in sickle-cell disease. Nat Med. 2002; 8:1383–1389. [PubMed: 12426562]

Sivamurthy KM, Dampier C, MacDermott M, Maureen M, Cahill M, Hsu LL. Peripheral arterial tonometry in assessing endothelial dysfunction in pediatric sickle cell disease. Pediatr Hematol Oncol. 2009; 26:589–96. [PubMed: 19954369]

Yuditskaya S, Tumblin A, Hoehn GT, Wang G, Drake SK, Xu X, Ying S, Chi AH, Remaley AT, Shen RF, Munson PJ, Suredini AF, Kato GJ. Proteomic identification of altered apolipoprotein patterns in pulmonary hypertension and vasculopathy of sickle cell disease. Blood. 2009; 113:1122–8. [PubMed: 19023114]

**Highlights**

- Sickle cell disease causes vascular dysfunction that increases mortality.

- We used infrared imaging of the skin to characterize vascular function.

- Skin temperature correlated with blood flow at rest and in response to vasodilators.

- Sickle cell patients with warm skin exhibited diminished responses to nitric oxide.

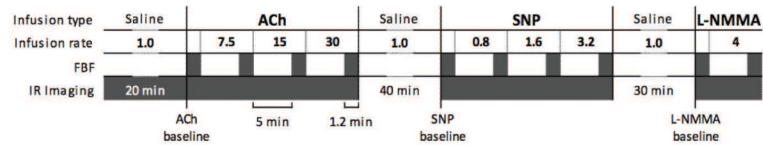- Warm skin may be a marker of vascular risk in patients with sickle cell disease.

**Figure 1. The sequence of vasoactive infusions, forearm blood flow measurements and infrared image acquisitions**

ACh, acetylcholine (infusion rate is in $\mu$g/min); SNP, sodium nitroprusside ($\mu$g/min); L-NMMA, L-$N^G$-monomethyl arginine ($\mu$mol/min); saline was infused at a rate of 1 mL/min. FBF, forearm blood flow; FBF was measured at baseline and before each dose escalation (shaded rectangles). Infrared images were acquired continuously except during the second and third saline infusions when the subject was allowed greater freedom of movement. Baseline forearm skin temperature and baseline forearm blood flow were measured before the start of each vasoactive infusion.
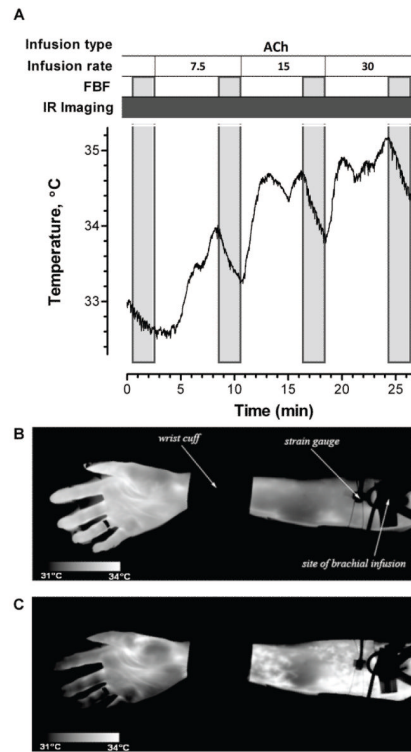
**Figure 2. Temperature profile and infrared images in one subject during ACh infusion**
**A**, ACh was infused at escalating rates of 7.5, 15, and 30 $\mu$g/min. FBF was measured at baseline and before each ACh infusion rate increase. Infrared (IR) images were acquired continuously. The region of interest used to calculate forearm skin temperature was between the wrist cuff and the strain gauge. **B**, An IR image of the subject's forearm during saline infusion. **C**, An IR image during ACh infusion. Increased skin temperature was immediately apparent in the real-time IR images during ACh infusion.
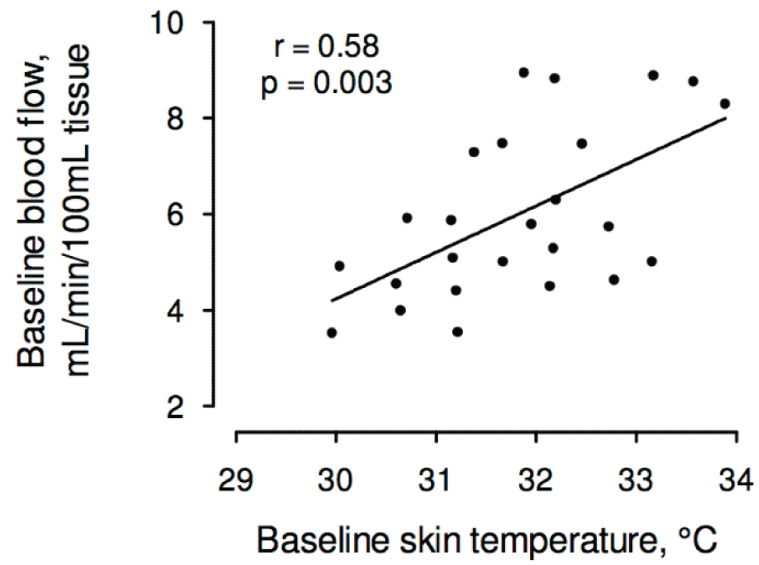
**Figure 3. The correlation between baseline forearm skin temperature and baseline forearm blood flow**

Baseline forearm skin temperature was correlated with baseline blood flow, $r = 0.58$, $p = 0.003$. Both measurements were taken prior to administration of any vasoactive drugs.
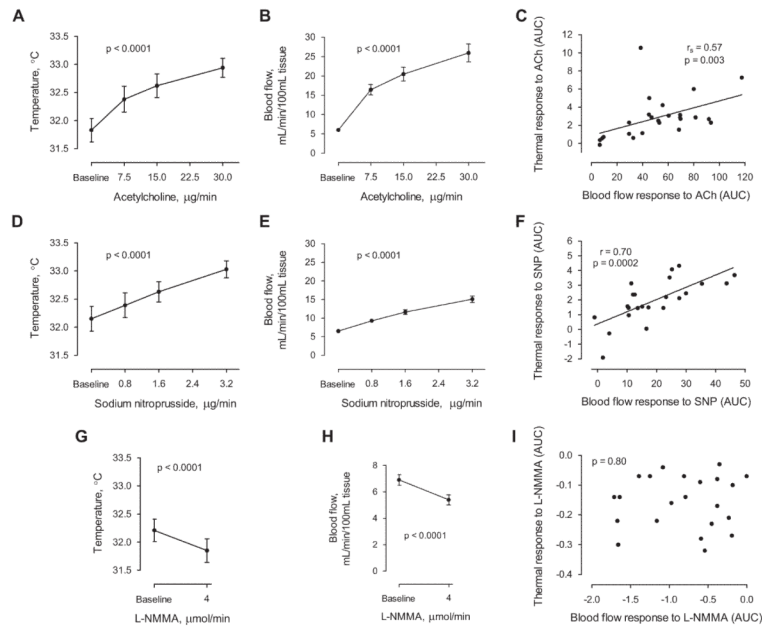
**Figure 4. Forearm skin temperature and forearm blood flow responses to vasoactive drug infusions**

**A**, Forearm skin temperature increased during ACh infusion. **B**, Forearm blood flow increased during ACh infusion. **C**, The area under the curve (AUC) of the thermal response to ACh was correlated with the AUC of the blood flow response to ACh. **D**, Forearm skin temperature increased during SNP infusion. **E**, Forearm blood flow increased during SNP infusion. **F**, The AUC of the thermal response to SNP was correlated with the AUC of the blood flow response to SNP. **G**, Forearm skin temperature decreased during L-NMMA infusion. **H**, Forearm blood flow decreased during L-NMMA infusion. **I**, The AUC of the thermal response to L-NMMA was not correlated with the AUC of the blood flow response to L-NMMA.
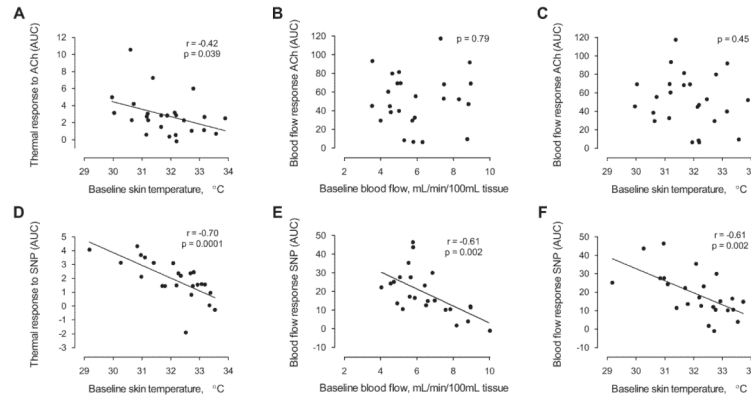
**Figure 5. The relationship between baseline forearm skin temperature and the forearm blood flow response to vasodilators**

**A**, Baseline forearm skin temperature measured before the start of the ACh infusion was inversely correlated with the area under the curve (AUC) of the thermal response to ACh; however, **B**, baseline forearm blood flow was not correlated with the AUC of the blood flow response to ACh. **C**, Baseline forearm skin temperature was not correlated with the AUC of the blood flow response to ACh. **D**, Baseline forearm skin temperature measured before the start of the SNP infusion was inversely correlated with the AUC of the thermal response to ACh. **E**, Baseline forearm blood flow was also inversely correlated with the blood flow response to SNP. **F**, Baseline forearm skin temperature was inversely correlated with the blood flow response to SNP. The $r$-statistic and $p$-value are coincidentally the same in Figures E, F.

**Comparison of Thermal and Blood Flow Responses to Maximum Dose SNP and ACh**
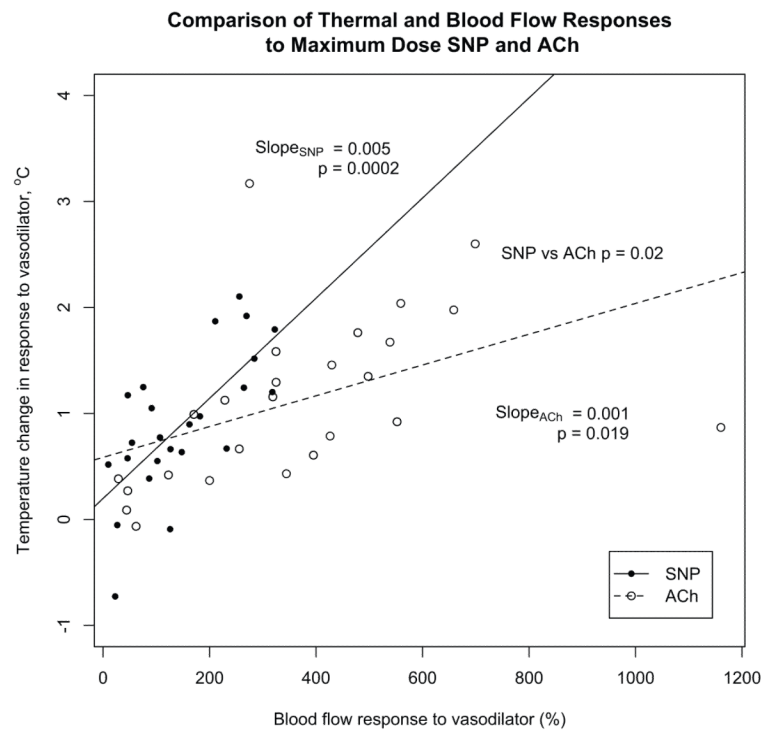
**Figure 6. A comparison of skin temperature and blood flow responses to vasodilators**
SNP elicited a greater skin temperature change than did ACh relative to the change in blood
flow ($p = 0.02$ by two-way ANOVA). This is indicated by the steeper slope of the regression
line relating the skin temperature change to the blood flow response for SNP (filled circles)
than for ACh (open circles).

**Table 1**

**Characteristics of the Study Population**

|  | Mean | SD |
|---|---|---|
| Age, years | 28 | 8 |
| Height, cm | 171 | 9 |
| Weight, kg | 68 | 17 |
| Females / Males | 10 / 15 |  |
| Diastolic blood pressure, mm Hg | 67 | 9 |
| Total hemoglobin, g/dL | 8.8 | 1.2 |
| White blood cell count, 1000/$\mu$L | 8.3 | 2.0 |
| Platelet count, 1000/$\mu$L | 358 | 180 |
| Lactate dehydrogenase, U/L | 322 | 105 |
| Creatinine, mg/dL | 0.6 | 0.2 |
| Total bilirubin, mg/dL | 3.7 | 2.0 |
| Direct bilirubin, md/dL | 0.5 | 0.3 |
| AST, units/L | 35 | 19 |
| ALT, units/L | 27 | 14 |
| INR | 1.2 | 0.1 |
| Cholesterol, mg/dL | 109 | 25 |
| Homocysteine, $\mu$mol/L | 7.9 | 2.2 |
| Total creatine kinase, units/L | 63 | 29 |
| N-terminal pro-brain natriuretic peptide, pg/mL | 81 | 79 |
| Tricuspid regurgitant velocity, m/s | 2.2 | 0.3 |

SD, standard deviation; AST, aspartate aminotransferase; ALT, alanine aminotransferase; INR, international normalized ratio.

**Table 2**

**Multivariable Linear Regression of Patient Characteristics Independently Associated with Baseline Forearm Skin Temperature**

| Variable | Coefficient | 95% CI | $P$ |
|----------|-------------|--------|-----|
| TRV | 9.6 | 3.9, 15.2 | 0.003 |
| Total hemoglobin | 1.8 | 0.4, 3.1 | 0.01 |
| Diastolic blood pressure | 0.07 | 0.04, 0.11 | 0.0006 |
| Homocysteine | −0.21 | −0.32, −0.10 | 0.001 |
| Cholesterol | −0.02 | −0.03, −0.001 | 0.03 |
| Interaction of hemoglobin and TRV | −1.0 | −1.1, −0.3 | 0.005 |

$R^2 = 0.84$, $F = 12.6$, $p < 0.0001$

TRV, Tricuspid valve regurgitant velocity.